Reprinted from

JAPANESE JOURNAL OF
APPLIED
PHYSICS

REGULAR PAPER

Unidirectional Liquid Crystal Pretilt Generation on Asymmetric Nanoscaled Groove Pattern Driven by Atomic Force Microscopic Tip

Jin Seog Gwag, Soo In Jo, You-Jin Lee, and Jae-Hoon Kim

Jpn. J. Appl. Phys. **51** (2012) 045203

Japanese Journal of Applied Physics **51** (2012) 045203 **REGULAR PAPER**
DOI: 10.1143/JJAP.51.045203

Unidirectional Liquid Crystal Pretilt Generation on Asymmetric Nanoscaled Groove Pattern Driven by Atomic Force Microscopic Tip

Jin Seog Gwag[1], Soo In Jo[2], You-Jin Lee[3], and Jae-Hoon Kim[2,3]*

[1]*Department of Physics, Yeungnam University, Gyeongsan, Gyeongbuk 712-749, Korea*
[2]*Department of Electronic Engineering, Hanyang University, Seoul 133-791, Korea*
[3]*Department of Information Display Engineering, Hanyang University, Seoul 133-791, Korea*

Received December 6, 2011; accepted February 11, 2012; published online April 2, 2012

We demonstrate uniformly and unidirectionally distributed pretilt characteristics of a liquid crystal cell fabricated via a substrate with a scan-directional slant nanosized surface groove pattern driven through an atomic force microscopic (AFM) tip that is continuously modulating the contact force in the scanning line direction. The resultant electro-optic characteristics of the liquid crystal (LC) cell made by our advanced AFM lithography technique show that it generates a unidirectional pretilt that guarantees wider LC applications.

1. Introduction

The surface alignment of liquid crystal (LC) molecules is a crucial factor considering the electro-optical properties of an LC device. In a general homogeneous LC cell, several surface LC alignment techniques with high productivity including the rubbing method have been presented to produce anisotropy on the LC alignment layer.[1–8] However, few methods can simply control the surface condition at the nano-scale, which greatly influences LC behavior.[7–10] Atomic force microscopy (AFM) nanolithography has emerged as an important research area capable of producing nanoscale-surface undulation for LC alignment.[11,12] And it is well known that directors of liquid crystal have a tendency to align parallel to the groove-shaped solid surface.[13] However, such surface undulation cannot produce LC pretilt due to the symmetric surface morphology. Thus, its use is limited to LC cells with horizontal switching, since zero pretilt gives rise to LC disclination formation in LC cells with vertical switching. Recently, in order to solve this pretilt problem, Tsui *et al.* have suggested an LC device with uniformly distributed submicron patterns by AFM.[14,15] However this method does not produce unidirectional pre-tilt, since there is no preferred direction between both alignments (x or $-x$ directions) even though LCs have bidirectional pre-tilt. Furthermore, little has been reported on the voltage-dependence-transmittance characteristics of LC cells fabricated to examine whether such surface morphologies produce LC disclination formation when voltage is applied to an LC cell. This would indicate whether LC pretilt is negligible.

In this letter, to expand the application of AFM lithography, we demonstrated twisted nematic (TN) cells with uniformly and unidirectionally distributed pretilt angle using a scan-directional slant nanosized-groove pattern scraped by an AFM tip with continuously modulated contact force in the scanning line. And we observed the electro-optic characteristics of LC cells made by our technique in order to confirm the unidirectional pretilt generation that guarantees wider LC applications.

2. Experiment

An ITO glass was spin-coated with a layer of polyimide (Nissan Chemical SE7492), which is currently used for homogeneous alignment, and its pretilt angle was 5°. And another homogeneous polyimide (Nissan Chemical RN1199) that has zero pretilt angle was used to confirm the pretilt angle created by AFM nanolithography. Each glass was spin-coated at 1000 rpm for 10 s and 2500 rpm for 10 s as the first and second step, respectively. And it was pre-baked at 100 °C for 10 min to remove the solvent and subsequently hard-baked at 210 °C for 1 h on a hot plate to completely polymerize it. The AFM nanolithography process was performed by commercial AFM (Park System XE-100) using the contact mode with various load forces. A diamond coated cantilever (905U-DT-NCHR) was used and its radius of apex is almost 20–30 nm. Using this AFM nanolithography process, we produced nano-scaled surface morphology whose size was $50 \times 50\,\mu m^2$ on the LC alignment layer. The big difference between our AFM nanolithography process and the conventional one[14,15] is the scan-directional slant nanosized surface groove pattern driven through the atomic force microscopic tip that is continuously modulating the contact force in the scanning line direction.

3. Results and Discussion

In order to examine the LC alignment in conventional AFM nanolithography producing constant amplitude, we made a directional linear pattern by the AFM contact mode with a cantilever force of 4000 nN. Generally, in this surface configuration, an azimuthal surface anchoring at A, the amplitude of the modulations is dominated simply by Berreman's theory, written as[13]

$$W_A = \frac{1}{2} K A^2 q^3 \quad (1)$$

where q is the wave number defined as $q = 2\pi/\lambda$ (λ is the groove pitch) and K is the elastic constant of LC. Figure 1 shows the AFM image of the surface morphology formed by conventional AFM nanolithography with a constant force. The pitch and depth of the surface morphology were 1 μm and about 20 nm, respectively. In that case, the azimuthal anchoring strength obtained from eq. (1) is $\sim 3 \times 10^{-6}$ N/m. The patterned polyimide substrate with the indium tin oxide (ITO) electrode was assembled with a counter ITO substrate coated by the same polyimide rubbed perpendicular to the AFM nanolithography direction in order to fabricate

*E-mail address: jhoon@hanyang.ac.kr

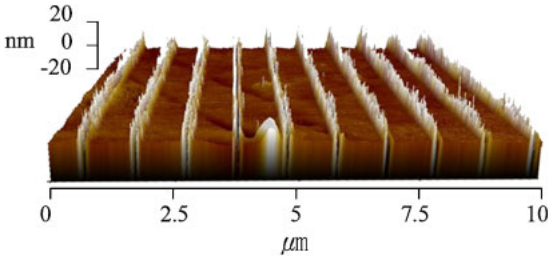

Fig. 1. (Color online) Topological AFM image of lithographed area.

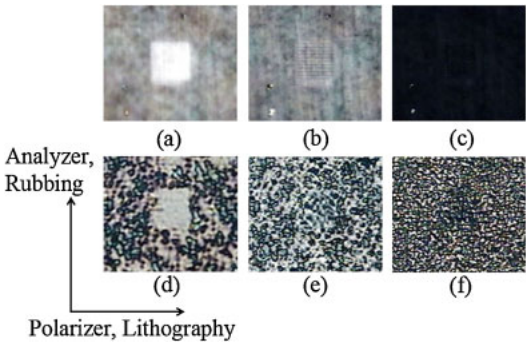

Fig. 2. (Color online) Optical microscope images of TN cells according to field under crossed polarizers; at (a) 0, (b) 3, and (c) 6 V of TN cell with SE7492 and at (d) 0, (e) 3, and (f) 6 V of TN cell with RN1199.

90° TN cells. LCs (MAT-03-382) were injected into the sandwich cell with a cell gap of 4.5 μm in the nanolithography direction, and the cell was sealed by a UV curable sealant. Figure 2 consists of microscopic images showing the electro-optical changes of the TN cells fabricated in the above manner under crossed polarizers. The upper three images show microscopic images of TN cells fabricated with SE-7492 polyimide generating a pretilt angle of 5°. Due to the LC pretilt angle of the rubbed substrate, no disclination lines can be observed, as shown in Figs. 2(b) and 2(c), when voltage is induced for the cell. On the other hand, the lower three images show microscopic images of TN cells fabricated with RN-1199 polyimide producing zero LC pretilt. In this case, however, many declination lines occur with an applied field, as shown in Figs. 2(e) and 2(f). These results obviously imply that the surface relief generated by conventional AFM nanolithography does not lead to the pretilt angle of LC.

In order to produce the pretilt angle by AFM lithography, we propose an improved line structure with continuously variable amplitude as shown in Fig. 3(a) which is schematic of the proposed line structure. Figure 3(b) is an AFM image of the proposed line structure. This structure is produced by continuously modulating the force of the AFM tip from start to end in the period of the AFM scanning process. In our experiment, the start force is set to 150 nN as the reference force of the contact mode, and the end force is set to 4000 nN. The scan rate of the AFM tip is 10 nm/s. In this surface configuration, if we assume the groove length is very long compared to the groove pitch, the azimuthal surface anchoring may be determined by the mean amplitude, written as

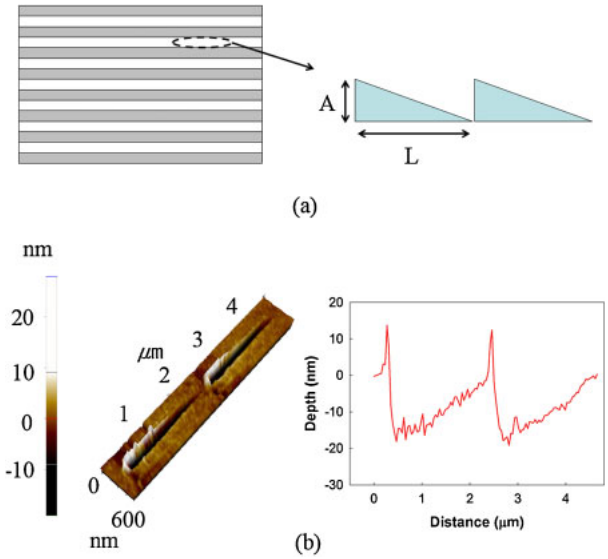

Fig. 3. (Color online) Schematic (a) and topological AFM image (b) of proposed slant groove structure.

$$W = \frac{1}{L}\int_0^L \frac{1}{2} Kq^3 a^2\, da = \frac{1}{6}\frac{A}{L} Kq^3 A^2 = \frac{1}{3}\frac{A}{L} W_A \quad (2)$$

where $a = l, \tan\varphi = l(A/L)$. Here, a, L, A, and φ are arbitrary amplitude in the scan direction, the pitch in the scan direction, maximum amplitude, and the sloop angle, respectively. If $\varphi = 45°$ or $A = L$, $W = (1/3)W_A$. The period of the scan direction and the groove pitch of the lithographed pattern are 2 and 1 μm, respectively. The depth varies from 0 to 20 nm and the sloop of this piece is 0.01, as shown in Fig. 3. Then, the azimuthal anchoring strength obtained from eq. (2) is $\sim 10^{-8}$ N/m, which is very weak anchoring. In this line structure, LC director will arrange toward the slant line. The total free energy per unit area, F_t can be expressed as the sum of the bulk elastic energy, F_b and the surface anchoring energy, F_s as follows:[14–17]

$$\begin{aligned} F_t = F_b + F_s = \frac{1}{2}\int [K_1(\nabla\cdot\boldsymbol{n})^2 + K_2(\boldsymbol{n}\cdot\nabla\times\boldsymbol{n})^2 \\ + K_3(\boldsymbol{n}\times\nabla\times\boldsymbol{n})^2]\, dr \\ + \frac{1}{2} W_{p2}\sin^2\theta + \frac{1}{4} W_{p4}\sin^4\theta \\ + \frac{1}{2} W_a \cos^2\theta \sin^2\phi(x,y), \end{aligned} \quad (3)$$

where n is the LC director, and K_1, K_2, and K_3 are, respectively, the splay, the twist, and the bend elastic constants. θ and ϕ are the polar and azimuthal angles of LCs, respectively. Here, W_p and W_a stand for the polar anchoring strength and the azimuthal anchoring strength of LC on substrate, respectively. Generally, W_{p2} is much smaller than W_{p4}. So here, W_{p2} is neglected. Then, with putting $W_{p4} \simeq 10^{-5}$ N/m which is a typical value for a polyimide, through minimization calculation of eq. (3), we expect that the surface morphology by our advanced AFM lithography will produce the pretilt angle of about 23° that agrees to ref. 15. Therefore, when voltage is induced to the sample, we expect disclination line doesn't occur in the lithography area unlike previous one.

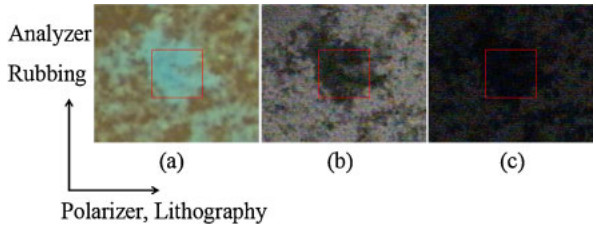

Fig. 4. (Color online) Optical microscope texture image of the TN cell fabricated by the advanced lithography technique on RN-1199 under crossed polarizers; at (a) $V = 0$, (b) 3, and (c) 6 V.

Figure 4 is the microscopic images showing the electro-optical changes of TN cells using our advanced AFM lithography technique on RN-1199. Transmissive color in the general 90° twisted nematic cell under cross polarizers is white, but in this case it is green due to the very weak anchoring strength of the lithographed substrate. To find the LC pretilt angle in the proposed pattern through the optical color of Fig. 4(a), we use the optical transmission equation in a twisted nematic LC cell given by[18,19]

$$T = \left[\cos\alpha\cos(\phi-\varphi_{\mathrm{p}}) + \frac{\phi_{\mathrm{r}}}{\alpha}\sin\alpha\sin(\phi-\varphi_{\mathrm{p}})\right]^2 + \frac{\beta^2}{\alpha^2}\sin^2\alpha\cos^2(\phi+2\varphi_0-\varphi_{\mathrm{p}}), \quad (4)$$

where ϕ is twist angle, φ_{p} is the angle between the transmission axes of input and output polarizers, φ_0 is the angle between transmission axis of input polarizer and input LC director, and $\alpha = (\phi_{\mathrm{r}}^2+\beta^2)^{1/2}$, $\beta = \pi d\Delta n(\theta)/\lambda$,

$$\Delta n(\theta) = \frac{1}{d}\int_0^d \frac{n_{\mathrm{e}}n_{\mathrm{o}}}{\sqrt{n_{\mathrm{e}}^2\sin^2\theta + n_{\mathrm{o}}^2\cos^2\theta}}\,dz - n_{\mathrm{o}}. \quad (5)$$

Here θ is the pretilt angle, λ is the wavelength of light source, d is cell gap, and n_{e} and n_{o} are the extraordinary and ordinary refractive indices of the LC material, respectively. In order to get twist angle of the LC cell, we use the general torque balance equation obtained by minimizing total free energy density. Then, in the asymmetrical structure like our cell structure with top substrate of very strong anchoring strength, the surface anchoring strength, W can be approximately written as

$$W_{\mathrm{asy}} = \frac{2K_{22}}{\sin(\Delta\phi_{\mathrm{asy}})}\frac{\phi}{d} = \frac{2K_{22}}{\sin\frac{1}{2}(2\phi_{\mathrm{e}}-\phi)}\frac{\phi}{d}, \quad (6)$$

where ϕ_{e} is the angle between the easy axes of the two substrates and $\Delta\phi_{\mathrm{asy}}$ is the angle at which the surface LC deviates from the easy axis which is the groove direction. Here, K_{22} and d of LC used are $\sim 10^{-12}$ Pa and 4.5 μm, respectively. Then, the twist angle obtained by azimuthal anchoring strength ($\sim 10^{-8}$ N/m) of the groove pattern from eq. (6) is *ca.* 11°. When putting this into eq. (4), the approximate pretilt angle corresponding to the spectrum of Fig. 4(a) is about 13°. This is in an acceptable result even though the pretilt result has some difference with it (23°) obtained from eq. (3) because this is the average value considering the top substrate having the pretilt angle of 0°. Compared with the previous data, we can easily establish that no disclination lines of the lithographed area occur in Figs. 4(b) and 4(c) with voltage. Consequently, we know the liquid crystal director of the lithographed area is arranged in a unique direction when voltage is induced. This result indicates that the pretilt angle of LC can be controlled by the proposed AFM technique. We expect that this technique will be useful to control surface LC behavior.

4. Conclusions

In summary, for complementing current AFM lithography techniques that do not generate unidirectional pretilt angle, we proposed a new lithography technique that produces a periodic slant groove structure. This can generate the pretilt angle and is induced through an AFM tip that is continuously modulating the contact force in the scanning line direction. And we confirmed pretilt generation in the proposed AFM lithography technique through observing the changes in macroscopic texture according to the voltage of the TN LC cell. This showed non-disclination formation of LC, indicating unidirectional pretilt generation. Our advanced AFM lithography technique may guarantee wider LC applications.

Acknowledgments

This work was supported by the National Research Foundation of Korea (NRF) grant funded by the Korea government (Grant No. 2011-0005327), and the Human Resources Development Program (R&D Workforce Cultivation Track for Solar Cell Materials and Processes) of Korea Institute of Energy Technology Evaluation and Planning (KETEP) grant (No. 20104010100580) funded by the Korea Ministry of Knowledge Economy.

1) W. M. Gibbons, P. J. Shannon, S. T. Sun, and B. J. Swetlin: Nature **351** (1991) 49.
2) N. Kawatsuki, T. Yamamoto, and H. Ono: Appl. Phys. Lett. **74** (1999) 935.
3) J.-H. Kim, S. Kumar, and S.-D. Lee: Phys. Rev. E **57** (1998) 5644.
4) M. Schadt, H. Seiberle, and A. Schuster: Nature (London) **381** (1996) 212.
5) P. Chaudhari: Nature (London) **411** (2001) 56.
6) J. L. Janning: Appl. Phys. Lett. **21** (1972) 173.
7) J. S. Gwag, J. Fukuda, M. Yoneya, and H. Yokoyama: Appl. Phys. Lett. **91** (2007) 073504.
8) J. S. Gwag, M. Yoneya, H. Yokoyama, and J.-H. Kim: Appl. Phys. Lett. **92** (2008) 153110.
9) J. A. Castellano: Mol. Cryst. Liq. Cryst. **94** (1983) 33.
10) C.-J. Yu, D.-W. Kim, and S.-D. Lee: Appl. Phys. Lett. **85** (2004) 22.
11) J. H. Kim, M. Yoneya, J. Yamamoto, and H. Yokoyama: Nanotechnology **13** (2002) 133.
12) A. J. Pidduck, G. P. Bryan-Brown, S. Haslam, R. Bannister, I. Kitely, T. J. McMaster, and L. Boogaard: J. Vac. Sci. Technol. A **14** (1996) 1723.
13) D. Berreman: Phys. Rev. Lett. **28** (1972) 1683.
14) B. Zhang, F. K. Lee, O. K. C. Tsui, and P. Sheng: Appl. Phys. Lett. **91** (2003) 215501.
15) F. K. Lee, B. Zhang, P. Sheng, H. S. Kwok, and O. K. C. Tsui: Appl. Phys. Lett. **85** (2004) 5556.
16) J.-H. Kim, M. Yoneya, J. Yamamoto, and H. Yokoyama: Mol. Cryst. Liq. Cryst. **367** (2001) 151.
17) H. Yokoyama and H. A. van Sprang: J. Appl. Phys. **57** (1985) 4520.
18) H. S. Kwok: J. Appl. Phys. **80** (1996) 3687.
19) J. S. Gwag, J. Yi, and J. H. Kwon: Opt. Lett. **35** (2010) 456.